Characterisation of Cortical Bone Adaptation: Mouse Tibia Loading Model

Corey Miller[1], Silvia Trichilo[2], Saulo Martelli[3], Peter Delisser[4], Lee B. Meakin[4], Joanna S. Price[4], Lance E. Lanyon[4], Peter Pivonka[1,2]

[1]School of Chemistry, Physics and Mechanical Engineering, (QUT), [2]St. Vincent's Department of Surgery, University of Melbourne,

[3]Medical Device Research Institute, Flinders University, [4]School of Veterinary Sciences, University of Bristol

INTRODUCTION

Bone Remodelling and Adaptation

The growth of bones in humans and animals throughout life follows a direct response to the load and usage regularly applied. Typically, the bone modelling cycle follows a well understood process outlined by Wolff's Law; the bone strength-to mass relationship is optimised such that the mechanical strain in the bone remains homeostatic [1].

Cortical bone's ability to adapt to an increase in dynamic loading has been analysed and the processes are well understood [2] [3]. Increases in both load and intensity of activity leads to additional bone formation, while disuse causes higher levels of resorption (Fig. 1). Recent studies in rats and mice have shown that the rate of formation and resorption has a linear relationship with the applied loading magnitude [5].

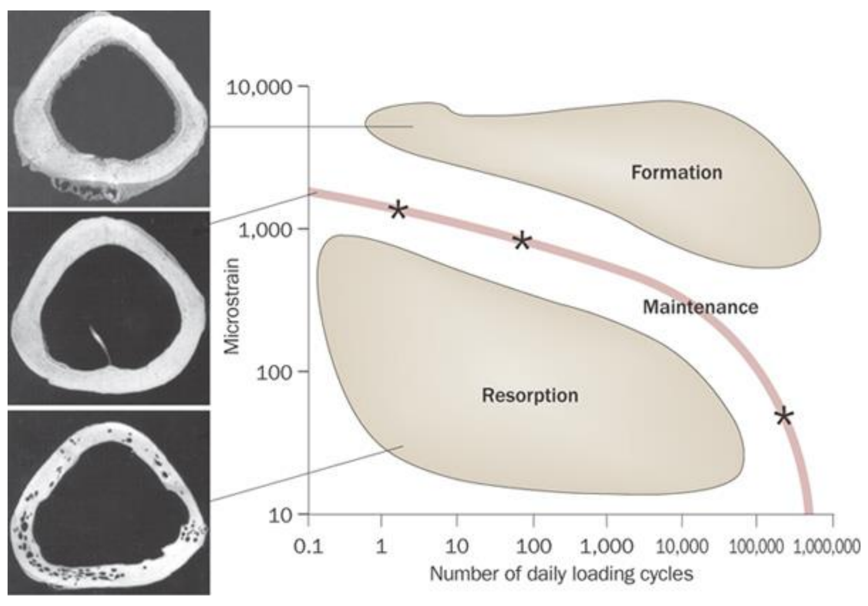

Fig. 1: Bone undergoes maintenance during regular activity, in accordance with Wolff's law. Strenuous or highly frequent loading cycles lead to an increase in bone formation, whereas less-intense, infrequent use causes bone to experience increased rates of resorption [4].

While cross-sectional area has been the standard metric of analysis in cortical bone, visual inspection of microCT images reveals that bone adaptation is localised to specific regions on the periosteum and is not uniform.

Objectives

The purpose of our research is to map the periosteal thickness of right tibiae loaded mice using a custom MATLAB image postprocessing algorithm, and to compare the loaded and control (i.e. left) limbs. This will provide novel insight into the localised bone adaptation response. The two major outcomes are:

(1) Determine the spatial location of localised adaptation responses on periosteal surfaces due to mechanical stimuli;
(2) Guide future research into developing bone adaptation algorithms, able to predict bone formation responses based on applied loading;

METHODOLOGY

Mouse Tibia Loading Tests

Our collaborators from the University of Bristol conducted experiments on 48 skeletally mature mice (17 weeks old), subjecting their right tibiae to repetitive loading on alternate days for two weeks [5]. The mice were grouped into categories based on peak dynamic loading cases, F = 0, 2, 4, 6, 8, 10, 12 and 14N, with six mice per category. At the conclusion of the experiment, mice were sacrificed and both left and right tibiae scanned using microCT imaging (Bruker, 1175, 4.75 μm resolution).

The mice tibia microCT image stack were normalised, and transverse slices were obtained for the 25%, 37%, 50% and 75% regions of the tibia (Fig. 2).

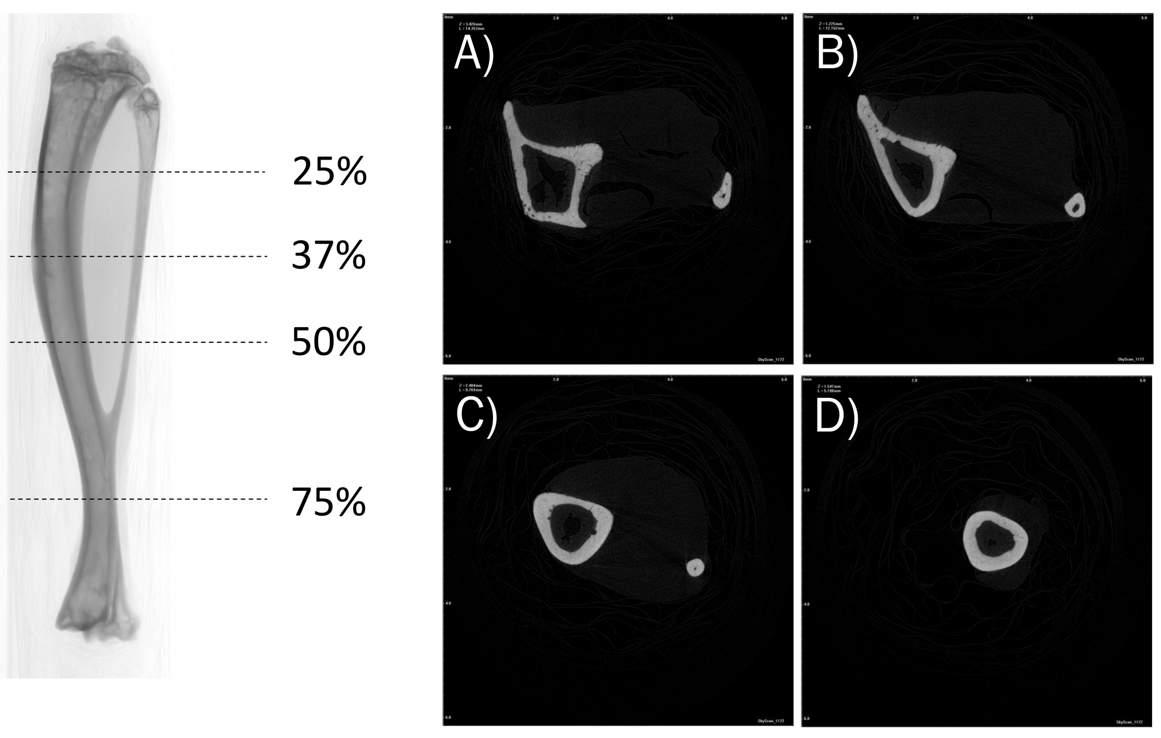

Fig. 2: MicroCT images of right mouse tibia at different cortical cross sections for F=12N: Left, longitudinal section of right tibia, labelled with the location slices used for image analysis. Right, Cross-sectional slices at: A) 25%, B) 37%, C) 50%, and D) 75%.

Image Processing in MATLAB

MicroCT images of the different sections (Fig. 2) are imported into MATLAB and converted into binary images. Small holes and local defects are filled in and smoothed in both the tibia and fibula. The custom image postprocessing algorithm consists of the following steps: *i:* determination of endosteal and periosteal surfaces $\rightarrow ii$: identify characteristic point on periosteum for alignment of right and left tibial thickness curves $\rightarrow iii$: computation cortical thickness (t) using two geometrical definitions $\rightarrow iv$: use of minimum thickness $\rightarrow v$: smoothing of thickness curve (Median & Butterworth filters) ; For effective comparison of left and right tibia thickness curves the periosteal length is normalized. Fig. 3 shows selected steps of the MATLAB image processing algorithm applied to the 25% proximal tibial slice (F=12N).

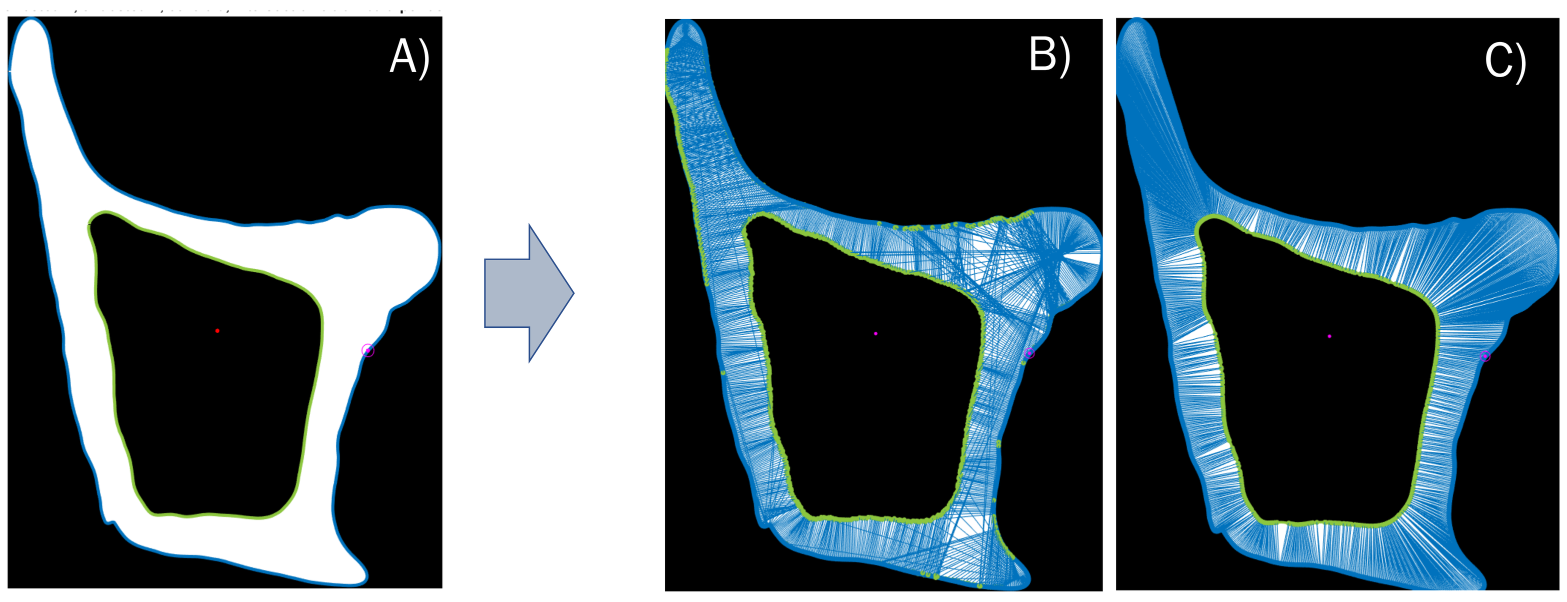

Fig. 3. Selected steps of MATLB image processing at the 25% proximal tibial slice (F=12N): *i:* identifying endosteal and periosteal surfaces (A); *iii:* two methods for computing cortical thickness, with one being calculating the minimum distance between endosteum and periosteum (B) and the second calculating the normal to the periosteal surface and finding the intersection point with the endosteum (C).

In order to compare right and left cortical thickness curves several strategies are used for alignment of curves. One strategy is based on anatomical considerations, i.e. finding the intersection of the line connecting area midpoints of tibia and fibula with the periosteal surface

RESULTS

The thickness measurements are conducted for each of the six mice per testing condition at the 25%, 37%, 50% and 75% tibial regions. The normalised thickness results are assessed using two-way ANOVA to ensure the differing thicknesses between the left and right tibias are statistically significant. Averaging and comparing the results per loading case and cross-sectional region shows several regions of increased thickness change along the cortical bone, with certain sections of the periosteum experiencing much greater thickness change than others (Fig. 5).

Fig. 4. Thickness comparison of the 0N, 2N and 12N dynamic loading cases at the 25% and 50% sections of the tibia.

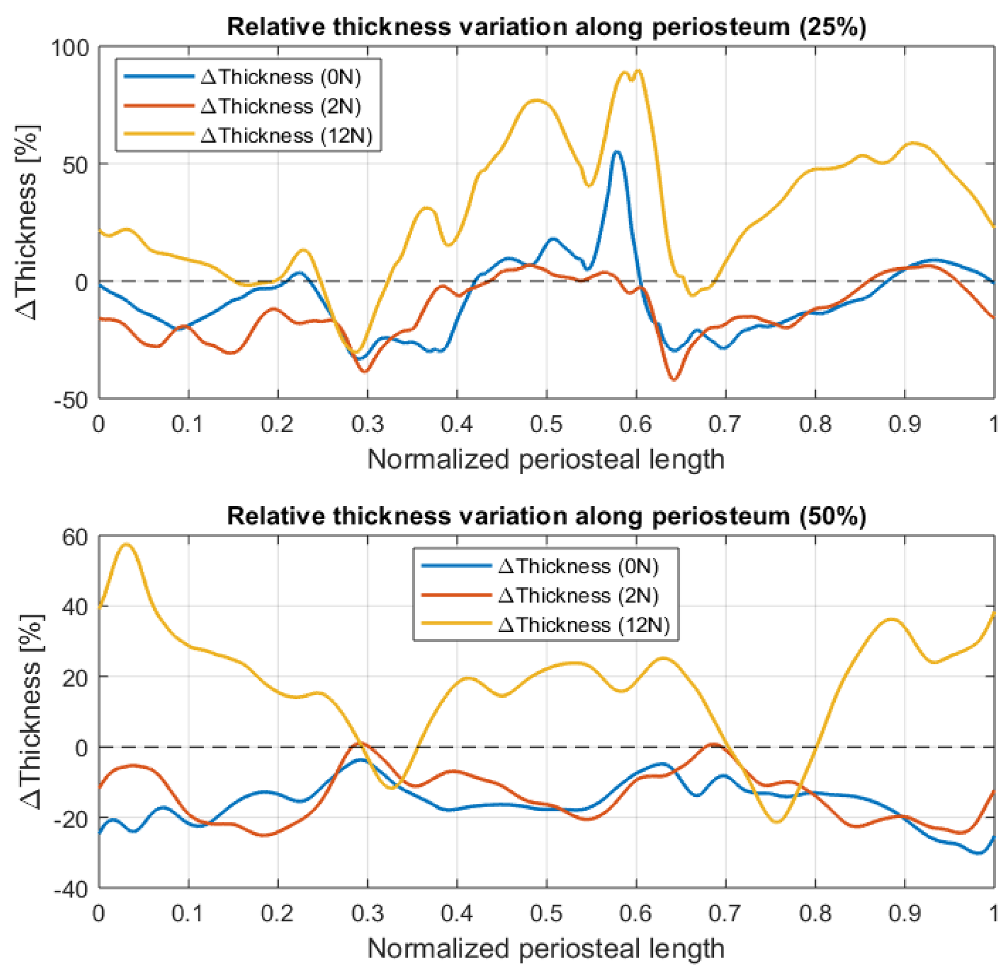

CONCLUSIONS & FUTURE WORK

Statistical analysis shows that bone adaption on periosteal surfaces is linked to the applied external load. In the future we will develop a finite element (FE) model to compute the strain energy density at the periosteal surface and investigate if the latter is related to localized bone adaptation response. Furthermore, we will develop adaptation algorithms predicting cortical thickness changes as function of the external loading regimen.

REFERENCES

[1] Wolff J. Das Gesetz der Transformation der Knochen (1892)
[2] Frost H.M. Journal of Bone and Mineral Research (1987), 2(2):73-85
[3] Turner C.H. Bone (1998), 23(5):399-407
[4] Qin Y.X. et al. Journal of Orthopaedic Research (1998), 16(4):482-9
[5] Sugiyama T. et al. Journal of Bone and Mineral Research (2012), 27(8):1784-1793R